Enhanced channel mobility of hexagonal boron nitride/hydrogen-terminated diamond heterojunction field-effect transistor

Yosuke Sasama,[1, a)] Takuya Iwasaki,[2] Masataka Imura,[3] Kenji Watanabe,[3] Takashi Taniguchi,[2] and Yamaguchi Takahide[2, 4]

[1)] *International Center for Young Scientists, National Institute for Materials Science, Tsukuba 305-0044, Japan*

[2)] *Research Center for Materials Nanoarchitectonics, National Institute for Materials Science, Tsukuba 305-0044, Japan*

[3)] *Research Center for Electronic and Optical Materials, National Institute for Materials Science, Tsukuba 305-0044, Japan*

[4)] *University of Tsukuba, Tsukuba 305-8571, Japan*

Hydrogen-terminated diamond field-effect transistors (FETs) using a hexagonal boron nitride (h-BN) gate insulator were fabricated on a diamond surface with reduced surface roughness in the direction of source/drain electrodes. The diamond surface was prepared on a mesa structure using chemical vapor deposition (CVD) with a low methane concentration. The hydrogen-terminated surface was laminated with the h-BN gate insulator without air exposure to prevent the adsorption of atmospheric surface acceptors. The hydrogen-terminated diamond FET exhibited a high mobility of $\approx$1000 $\mathrm{cm^2V^{-1}s^{-1}}$ at room temperature. We performed theoretical analysis on the temperature and carrier density dependences of mobility, which suggested that Coulomb and surface roughness scattering were effectively reduced. The high mobility obtained in this study indicates the high potential of diamond as a semiconducting material. This study can contribute to the future development of diamond devices.

[a)]SASAMA.Yosuke@nims.go.jp

Diamond is a wide-gap semiconductor with a high breakdown electric field, high thermal conductivity, and high mobility, making it advantageous for power device applications[1,2]. Several types of diamond field-effect transistors (FETs) have been developed, including Schottky metal-semiconductor FETs[3], junction FETs[4], and deep-depletion FETs[5]. One of the most widely developed FETs is the hydrogen-terminated diamond FET, in which the diamond surface is terminated with hydrogen[6]. This is because terminating the diamond surface with hydrogen reduces the surface state density, and the higher energy of the valence band maximum facilitates the induction of hole carriers[7].

Hydrogen-terminated diamond FETs often use the surface conductivity induced by transfer doping.[8] The surface conductivity can be obtained simply by exposing the hydrogen-terminated surface to air.[9] Additionally, carrier density can be increased to $>10^{14}$ cm^{-2} by exposure to NO_2 gas[10] or the deposition of oxides with a large electron affinity[11].

However, negative charges associated with the formation of surface conductivity on the hydrogen-terminated surface (ionized surface acceptors or atmospheric negative charges) scatter carriers and reduce the mobility of FETs. Reduced mobility is undesirable for high-speed and low-loss operation of FETs. To increase the mobility of diamond FETs, we have fabricated FETs with a reduced surface acceptor density using a hexagonal boron nitride (h-BN) gate insulator[12–14] and an air-free process[15], in which the hydrogen-terminated surface is not exposed to air. We have obtained a high mobility of 680 cm^{2}V^{-1}s^{-1} with a relatively high carrier density of 6.6×10^{12} cm^{-2}. In addition to the high mobility, the FETs also demonstrate normally off operation, low on-resistance, and high on-off ratio simultaneously.[15]

In this study, we made two primary improvements to further increase the mobility of diamond FETs. The first is the reduction of surface roughness on a diamond. Surface roughness can contribute to the formation of surface states[16]. Charges trapped at surface states cause Coulomb scattering, resulting in reduced mobility. Mobility is also reduced by surface roughness scattering. Here, we grew a relatively flat diamond film on a mesa structure using chemical vapor deposition (CVD) with a low methane concentration[17], and we fabricated FETs on the diamond film. The second improvement is the lamination technique of h-BN. Here, we use pick-up method to laminate h-BN. The use of this pick-up method[18,19] effectively avoids the formation of contamination bubbles, which are often problematic when creating van der Waals heterostructures. Through the use of a curvature polymer and slowly

laminating the layers, bubbles are pushed out, resulting in the formation of a clean interface free from contamination bubbles. Therefore, this method has been increasingly employed in recent years to fabricate van der Waals heterostructures[20], including recent h-BN/diamond hetero devices.[21,22]

First, we focused on the growth of diamond films. Generally, a diamond (111) substrate has a misorientation angle, and atomic steps exist on the substrate surface. When diamond is grown using CVD with a low methane concentration on a (111) diamond substrate, it grows laterally from atomic steps, and atomically flat diamond can be formed[17]. Following the previous report, we grew diamond films. We used type-Ib (111) single-crystalline diamond substrate manufactured by Sumitomo Electric Industries. After the mesa structure was formed on the diamond substrate using oxygen plasma etching, the diamond was grown using CVD under the following conditions: hydrogen flow rate of 1000 sccm, methane flow rate of 0.1 sccm, microwave power of 800 W, and pressure of 80 torr. The quality of the diamond surface was evaluated using an atomic force microscope (AFM). Measurements were performed on an area of 20 μm square. Steps existed in the direction perpendicular to the [111] direction, but a relatively flat diamond film with an average surface roughness (Ra) of $\approx$0.15 nm was grown (Fig. 1c).

Subsequently, we fabricated an FET using a h-BN gate insulator with a Hall-bar structure (Fig. 1a) on the CVD-grown diamond. First, Ti/Pt was deposited as electrodes. Here, the source/drain electrodes (current electrodes in the Hall bar) were placed parallel to the step of the diamond. An annealing was performed in a hydrogen atmosphere (hydrogen flow rate of 500 sccm, pressure of 80 torr) at 650°C for 35 min to form TiC, which functions as an ohmic electrode. Thereafter, the diamond surface was exposed to hydrogen plasma to remove resist residue and atmospheric adsorbates. The hydrogen plasma conditions were as follows: hydrogen flow rate of 500 sccm, microwave power of 300 W, pressure of 30 torr, and duration of 10 min. Annealing and hydrogen plasma treatment were also performed in another CVD chamber under the same conditions as in the first chamber. The second CVD chamber could be connected to a vacuum suitcase. The diamond was vacuum-transferred to an Ar-filled glove box using the vacuum suitcase to avoid the adsorption of atmospheric adsorbates on the hydrogen-terminated diamond surface. In the glove box, the hydrogen-terminated diamond was laminated with a cleaved h-BN thin film. Here, we used the pick-up method[18,19,21,22] for the h-BN transfer. A single-crystalline h-BN was cleaved with scotch

tape and transferred onto a Si substrate. The cleaved h-BN film was then picked up from the Si substrate using a polymer stamp and transferred onto the diamond. The lamination of diamond with h-BN was performed at room temperature and then the diamond was heated to 110°C to release the h-BN from the stamp. The thickness of the h-BN film used in this study was 16 nm. After the h-BN lamination, the diamond substrate was annealed in the glove box at 200°C for 3 h. The diamond substrate was then removed from the glove box. The h-BN gate insulator was etched into a Hall-bar shape using capacitively coupled plasma reactive ion etching (RIE) with N_2, CHF_3, and O_2 gases. The diamond surface, except for the area underneath the h-BN, was converted to oxygen termination during this process, providing device isolation. Subsequently, Ti/Au/Ti films were deposited on the h-BN as a gate electrode. The hydrogen-terminated diamond may attract negatively charged impurities, resulting in the intercalation of impurities at the interface between the diamond and h-BN, because the hydrogen-terminated diamond surface is slightly positively charged owing to the difference in electronegativity between carbon and hydrogen atoms[8]. To prevent impurities from contaminating the interface, we deposited 30-nm Al_2O_3 using atomic layer deposition. We consider that the Al_2O_3 passivation contributes to the long-term stability of the device. Thereafter, through holes were opened in Al_2O_3 using wet etching with dilute tetramethylammonium hydroxide. Finally, the gate contact was fabricated through the sputter deposition of Ti/Au. The optical microscope image of the fabricated device is shown in Fig. 1b.

We evaluated the electrical characteristics of the FET. Figure 2a shows the transfer characteristics. (See also Fig. S1 of the supplementary material.) The FET exhibits p-type FET characteristics. The maximum sheet conductance is 1.1 mS, which corresponds to a sheet resistance of 0.93 kΩ. The sheet conductance (σ) is obtained as $\sigma = (L_\mathrm{p}/W_\mathrm{G})(1/R)$, where R is the resistance measured using the four-terminal method, W_G (= 0.97 μm) is the gate width, and L_p (= 3.0 μm) is the distance between the voltage probes. This device has a fringe region in which the diamond surface is hydrogen-terminated and covered by h-BN, but it is not under the gate electrode. This region may be conductive owing to hole carriers generated by surface acceptors originating from residual gases in the glove box. The conductance in the fringe region may result in an overestimate of the sheet conductance. However, if we assume that the sheet conductance in the fringe region is equal to that in the gate-overlapped region at zero gate voltage, the impact of the fringe region on the maximum

sheet conductance is estimated to be only 7%. This value is obtained as $\Delta\sigma = \sigma(V_{\mathrm{GS}} = 0) \times (W_{\mathrm{h-BN}} - W_{\mathrm{G}})/W_{\mathrm{h-BN}}$ using the h-BN width ($W_{\mathrm{h-BN}} = 3.97$ μm) and gate width. The threshold voltage evaluated from the transfer curve is 0.67 V. Unlike our previous study, the threshold voltage is positive, which indicates normally on operation. We consider that the reason for this positive threshold voltage is a lower concentration of nitrogen[23] acting as a donor unlike in the previous one[15]. The diamond substrates used in our previous study were type-IIa high pressure, high temperature(HPHT)-grown diamond purchased from the Technological Institute for Superhard and Novel Carbon Materials (TISNCM), and secondary ion mass spectrometry (SIMS) on a similar substrate showed that the nitrogen concentration in the substrate was ≈500 ppb. In contrast, the nitrogen concentration in diamond grown under the similar conditions as in the present study was below the detection limit of SIMS measurement (<20 ppb).

Figure 2b shows the output characteristics. The drain-source length is 8.8 μm. The maximum drain current density is ≈240 mA mm^{-1}. The drain current density is obtained by dividing the drain current by the gate width. Based on a simple calculation considering the gate and h-BN width, the current flowing through the fringe region ($I(V_{\mathrm{GS}} = 0) \times ((W_{\mathrm{h-BN}} - W_{\mathrm{G}})/W_{\mathrm{h-BN}})$) is 15 mA mm^{-1}, which is as low as 6% of the maximum drain current density. The FET is not completely turned off because of the fringe current. Because the gate electrode does not cover the fringe region, the hole carriers do not deplete even when a positive gate voltage is applied. Therefore, a small drain current flows even when a positive gate voltage is applied. To completely turn off the FET, we believe that device isolation techniques should be improved.

Carrier density and mobility were evaluated using Hall-effect measurements. Figure 2c shows the gate voltage dependence of the carrier density. The carrier density increased monotonically, with a maximum carrier density of 4.7×10^{12} cm^{-2}. Figure 2d shows the Hall mobility. Field-effect mobility ($\mu_{\mathrm{FE}} = \frac{t_{\mathrm{hBN}}}{\epsilon_{\mathrm{hBN}}} \left|\frac{\partial\sigma}{\partial V_{\mathrm{GS}}}\right|$) and effective mobility ($\mu_{\mathrm{eff}} = \frac{t_{\mathrm{hBN}}}{\epsilon_{\mathrm{hBN}}} \frac{\sigma}{|V_{\mathrm{GS}} - V_{\mathrm{th}}|}$) estimated from the slope of the transfer characteristic (Fig. 2a) are also shown. σ is the sheet conductance shown in Fig. 2a, V_{GS} is the gate voltage, t_{hBN} is the thickness of h-BN, and $\epsilon_{\mathrm{hBN}} = 3$ is the dielectric constant of h-BN. For the estimation of Hall mobility, the conductance of the side paths was subtracted using the same method as in our previous work[12]. The Hall mobility (μ_{Hall}) is calculated as $\mu_{\mathrm{Hall}} = (\sigma - \sigma(V_{\mathrm{GS}} = 0)(W_{\mathrm{h-BN}} - W_{\mathrm{G}})/W_{\mathrm{h-BN}})/(n_{\mathrm{H}}e)$. σ is the sheet conductance, n_{H} is the Hall carrier density, and e is the elementary charge

(Figure S2 of the supplementary material). A high mobility of ≈1000 $cm^2V^{-1}s^{-1}$ was observed in the Hall, field-effect, and effective mobilities. The Hall mobility is slightly higher than effective and field-effect mobilities, which might be related to the current paths besides the channel. We note that we can rule out the possibility that the high mobility originates from boron contamination in the diamond film. The density of carriers induced by boron does not increase with increasing negative gate voltage; hence, at least the field-effect mobility is considered to be the mobility of a two-dimensional hole gas induced by applying a gate voltage on a hydrogen-terminated diamond.

We also evaluated the temperature dependence of the mobility. Figure 3 shows the temperature dependence of the mobility evaluated using Hall-effect measurements. The mobility of our present FETs fabricated on a CVD-grown diamond increases with decreasing temperature more rapidly than our previous FETs fabricated on a diamond surface without CVD growth. The maximum mobility is ≈2300 $cm^2V^{-1}s^{-1}$ at 100 K. Below 100 K, the mobility could not be evaluated accurately owing to the large contact resistance at low temperature. The large contact resistance at low temperatures may originate from the gap formed at the h-BN/diamond interface near the Hall-bar electrodes, as discussed in our recent paper[22]. The cleaner surface compared with before may increase the electrical resistance of diamond underneath the gap near electrodes and, therefore, the contact resistance at low temperatures. We consider that the use of gate electrode self-aligned with source/drain electrodes[22] can eliminate the gap formed at the h-BN/diamond interface near the electrodes and reduce the contact resistance.

The reduction of Coulomb and surface roughness scattering was supported by the theoretical analysis of mobility. Figure 4 shows the theoretical analysis of (a) carrier density dependence and (b) temperature dependence of mobility. (See also Fig. S3 of the supplementary material.) The mobility was calculated theoretically using the same method as in our previous report (Supplementary Information in Ref.[15]). As shown in Fig. 4, the theoretical calculations of mobility adequately explain the experimental results for both the carrier density and the temperature dependences of mobility. Here, the boron and nitrogen concentrations were set to 1 and 5 ppb, respectively, and the average roughness (Δ) was set to 0.15 nm based on AFM measurements. We have tuned the interfacial charge density (n_{ic}) and distance between the interfacial charges and hole carriers (d). The values of d and n_{ic} were determined by minimizing the total sum of squared residuals between the calculated

and experimental mobilities at $V_{GS} = -2, -4$ and -6 V. Consequently, the optimal values were found to be $d = 0.0$ nm and $n_{ic} = 2.4 \times 10^{11}$ cm^{-2}. The obtained value of d is consistent with those assumed in references[14],[15], and[25], and is similar to the value reported in reference[24]. The experimental results of our previous study[15] are well explained when the calculation parameter values are $n_{ic} = 6 \times 10^{11}$ cm^{-2}, $\Delta = 0.18$ nm, whereas the results of this study are well explained when the calculation parameter values are $n_{ic} = 2.4 \times 10^{11}$ cm^{-2}, $\Delta = 0.15$ nm. The reduction in n_{ic} is considered to be owing to both the decrease in the surface roughness and improvement in the h-BN lamination technique. The reduction in surface roughness is expected to decrease the density of the interface states. The use of the pick-up method for the h-BN lamination has also contributed to the improvement in mobility by reducing the charged impurity density at the hydrogen-terminated diamond/h-BN interface.

In summary, we fabricated diamond FETs using an h-BN gate insulator on a diamond film grown using CVD with a low methane concentration. Through the CVD with a low methane concentration, a diamond film with reduced surface roughness in the direction of source/drain electrodes was grown. The h-BN gate insulator was formed via the cleavage of h-BN and a pick-up method using a curvature polymer stamp. We demonstrated that a high hole mobility of $\approx$1000 cm^{2}V^{-1}s^{-1} can be achieved at room temperature in the hydrogen-terminated diamond FET by improving the quality of the interface between the hydrogen-terminated diamond and gate insulator. The theoretical analysis of the carrier density and temperature dependences of mobility supported that this high mobility was achieved by reducing surface roughness and interface charge density. This mobility approaches that of the electron mobility in GaN high electron mobility transistors (HEMTs), suggesting that combining our diamond FET with a GaN-HEMT can enable high-performance complementary circuits based on wide-bandgap semiconductors.

Supplementary Material

See the supplementary material for additional analysis on the FET's long-term electrical stability, calculation of Hall mobility accounting for fringe conductance, and the theoretical and experimental exploration of temperature-dependent mobility at various gate voltages.

Data availability

The data supporting the findings of this study are available from the corresponding author upon reasonable request.

REFERENCES

[1]N. Donato, N. Rouger, J. Pernot, G. Longobardi, and F. Udrea, "Diamond power devices: state of the art, modelling, figures of merit and future perspective," Journal of Physics D: Applied Physics **53**, 093001 (2020).

[2]D. Eon, "Diamonds in the current: Navigating challenges for the integration of diamond in power electronics," physica status solidi (a) **221**, 2400085 (2024).

[3]H. Kawarada, M. Aoki, and M. Ito, "Enhancement mode metal - semiconductor field effect transistors using homoepitaxial diamonds," Applied Physics Letters **65**, 1563–1565 (1994).

[4]T. Iwasaki, Y. Hoshino, K. Tsuzuki, H. Kato, T. Makino, M. Ogura, D. Takeuchi, T. Matsumoto, H. Okushi, S. Yamasaki, and M. Hatano, "Diamond junction field-effect transistors with selectively grown n+-side gates," Applied Physics Express **5**, 091301 (2012).

[5]T. T. Pham, J. Pernot, G. Perez, D. Eon, E. Gheeraert, and N. Rouger, "Deep-depletion mode boron-doped monocrystalline diamond metal oxide semiconductor field effect transistor," IEEE Electron Device Letters **38**, 1571–1574 (2017).

[6]H. Kawarada, "Hydrogen-terminated diamond surfaces and interfaces," Surface Science Reports **26**, 205–259 (1996).

[7]S. J. Sque, R. Jones, and P. R. Briddon, "Structure, electronics, and interaction of hydrogen and oxygen on diamond surfaces," Physical Review B **73**, 085313 (2006).

[8]H. Kawarada, "Diamond p-FETs using two-dimensional hole gas for high frequency and high voltage complementary circuits," Journal of Physics D: Applied Physics **56**, 053001 (2022).

[9]F. Maier, M. Riedel, B. Mantel, J. Ristein, and L. Ley, "Origin of surface conductivity in diamond," Physical Review Letters **85**, 3472–3475 (2000).

[10]M. Kasu, "Diamond field-effect transistors for RF power electronics: Novel NO_2 hole doping and low-temperature deposited Al_2O_3 passivation," Japanese Journal of Applied Physics **56**, 01AA01 (2017).

[11]S. A. O. Russell, L. Cao, D. Qi, A. Tallaire, K. G. Crawford, A. T. S. Wee, and D. A. J. Moran, "Surface transfer doping of diamond by MoO_3: A combined spectroscopic and Hall measurement study," Applied Physics Letters **103**, 202112 (2013).

[12]Y. Sasama, K. Komatsu, S. Moriyama, M. Imura, T. Teraji, K. Watanabe, T. Taniguchi, T. Uchihashi, and Y. Takahide, "High-mobility diamond field effect transistor with a monocrystalline h-BN gate dielectric," APL Materials **6**, 111105 (2018).

[13]Y. Sasama, K. Komatsu, S. Moriyama, M. Imura, S. Sugiura, T. Terashima, S. Uji, K. Watanabe, T. Taniguchi, T. Uchihashi, and Y. Takahide, "Quantum oscillations in diamond field-effect transistors with a h-BN gate dielectric," Physical Review Materials **3**, 121601(R) (2019).

[14]Y. Sasama, T. Kageura, K. Komatsu, S. Moriyama, J.-i. Inoue, M. Imura, K. Watanabe, T. Taniguchi, T. Uchihashi, and Y. Takahide, "Charge-carrier mobility in hydrogen-terminated diamond field-effect transistors," Journal of Applied Physics **127**, 185707 (2020).

[15]Y. Sasama, T. Kageura, M. Imura, K. Watanabe, T. Taniguchi, T. Uchihashi, and Y. Takahide, "High-mobility p-channel wide-bandgap transistors based on hydrogen-terminated diamond/hexagonal boron nitride heterostructures," Nature Electronics **5**, 37–44 (2022).

[16]M. Nagai, R. Yoshida, T. Yamada, T. Tabakoya, C. E. Nebel, S. Yamasaki, T. Makino, T. Matsumoto, T. Inokuma, and N. Tokuda, "Conductive-probe atomic force microscopy and kelvin-probe force microscopy characterization of OH-terminated diamond (111) surfaces with step-terrace structures," Japanese Journal of Applied Physics **58**, SIIB08 (2019).

[17]N. Tokuda, H. Umezawa, S.-G. Ri, M. Ogura, K. Yamabe, H. Okushi, and S. Yamasaki, "Atomically flat diamond (111) surface formation by homoepitaxial lateral growth," Diamond and Related Materials **17**, 1051–1054 (2008).

[18]F. Pizzocchero, L. Gammelgaard, B. S. Jessen, J. M. Caridad, L. Wang, J. Hone, P. Boggild, and T. J. Booth, "The hot pick-up technique for batch assembly of van der waals heterostructures," Nature Communications **7**, 11894 (2016).

[19]T. Iwasaki, K. Endo, E. Watanabe, D. Tsuya, Y. Morita, S. Nakaharai, Y. Noguchi, Y. Wakayama, K. Watanabe, T. Taniguchi, and S. Moriyama, "Bubble-free transfer technique for high-quality graphene/hexagonal boron nitride van der waals heterostructures," ACS Appl Mater Interfaces **12**, 8533–8538 (2020).

[20]W. Dong, Z. Dai, L. Liu, and Z. Zhang, "Toward clean 2D materials and devices: Recent progress in transfer and cleaning methods," Adv Mater , e2303014 (2023).

[21]Y. Huang, J. Xiao, R. Tao, Z. Liu, Y. Mo, X. Yu, Z. Cao, Y. Wu, Z. Li, H. Wang, and L. Wang, "High mobility hydrogen-terminated diamond FET with h-BN gate dielectric using pickup method," Applied Physics Letters **123**, 112103 (2023).

[22]Y. Sasama, T. Iwasaki, M. Monish, K. Watanabe, T. Taniguchi, and Y. Takahide, "Self-aligned gate electrode for hydrogen-terminated diamond field-effect transistors with a hexagonal boron nitride gate insulator," Applied Physics Letters **125**, 092103 (2024).

[23]T. Matsumoto, T. Yamakawa, H. Kato, T. Makino, M. Ogura, X. Zhang, T. Inokuma, S. Yamasaki, and N. Tokuda, "Fabrication of inversion p-channel MOSFET with a nitrogen-doped diamond body," Applied Physics Letters **119**, 242105 (2021).

[24]Y. Li, J.-F. Zhang, G.-P. Liu, Z.-Y. Ren, J.-C. Zhang, and Y. Hao, "Mobility of two-dimensional hole gas in H-terminated diamond," physica status solidi (RRL) - Rapid Research Letters **12**, 1700401 (2018).

[25]G. Daligou and J. Pernot, "2D hole gas mobility at diamond/insulator interface," Applied Physics Letters **116**, 162105 (2020).

Acknowledgments

We thank H. Osato, E. Watanabe, D. Tsuya, N. Ikeda, and A. Ohi for technical support. We thank T. Ando, S. Koizumi, and T. Teraji for their assistance with this study. This study was financially supported by the NEDO Uncharted Territory Challenge 2050 (Project No. JPNP14004), JSPS KAKENHI (Grant No. JP22H01962) and Advanced Research Infrastructure for Materials and Nanotechnology in Japan (ARIM) (Proposal No. JPMXP1224NM5213).

Competing Interests

The authors declare that they have no competing financial interests.

Data availability

The data that support the findings of this study are available from the corresponding author upon reasonable request.

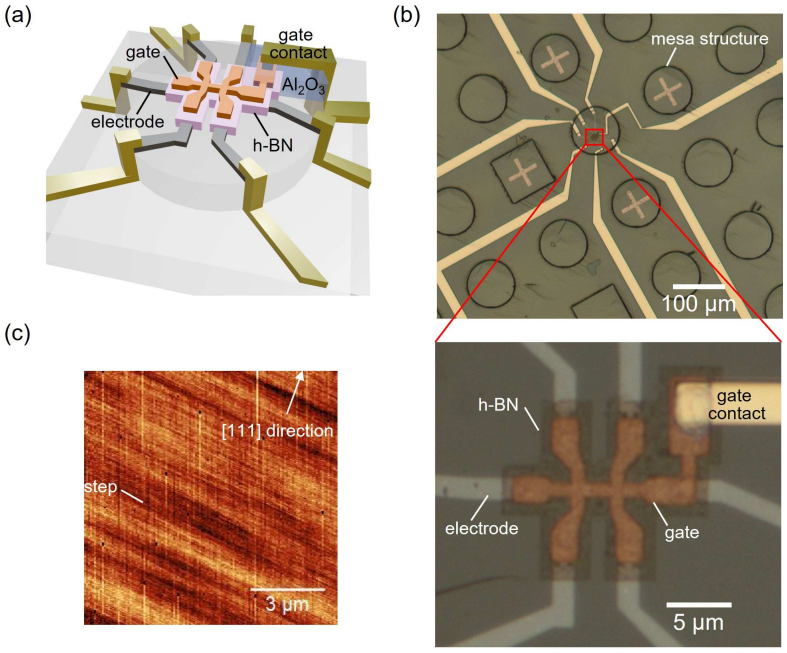

FIG. 1. (a) Schematic and (b) optical microscope image of the diamond FET fabricated in this study. (c) AFM image of the diamond surface after CVD growth. The arrow represents the projection of the [111] direction onto a two-dimensional plane.

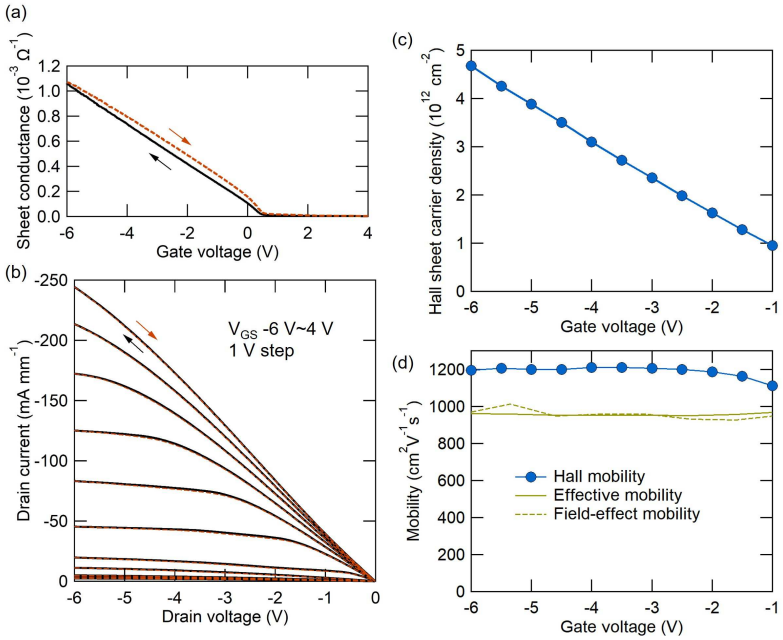

FIG. 2. Device characteristics of the diamond FET (Sample B1) at 300 K. (a) Transfer characteristics, (b) output characteristics, (c)(d) gate voltage dependence of (c) carrier density and (d) mobility.

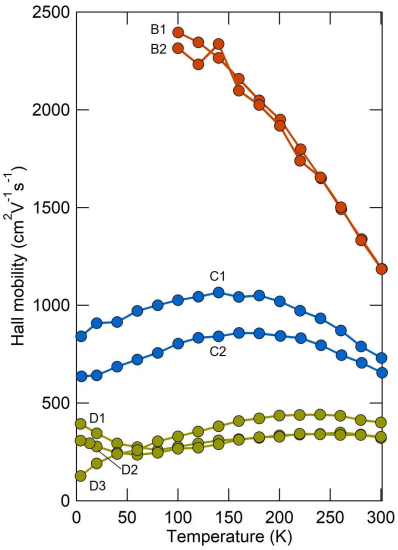

FIG. 3. Temperature dependence of Hall mobility. The points connected by lines are the measurement results of the same device measured at different temperatures. Samples B1 and B2 were fabricated on a CVD-grown diamond surface, whereas samples C1, C2 (ref.[15]) and D1-D3 (ref.[12]) were fabricated on a diamond surface without CVD growth. Samples B1, B2, C1, and C2 were fabricated without air exposure to hydrogen-terminated surface, whereas samples D1-D3 were fabricated on an air-exposed hydrogen-terminated surface. Measurements were performed with the application of a gate voltage (-6 V for B1, -15 V for B2, -8 V for C1, -10 V for C2, -4 V for D1, -7 V for D2, -5 V for D3, depending on the thickness of h-BN). Sample B2 exhibited fluctuations in electrical measurements at low temperatures owing to a high contact resistance. Sample B2 was fabricated using a process in which the gate electrode was self-aligned with source/drain electrodes. Some of the hydrogen-terminated surface in the access region was damaged during the h-BN etching process, resulting in high contact resistance in sample B2.

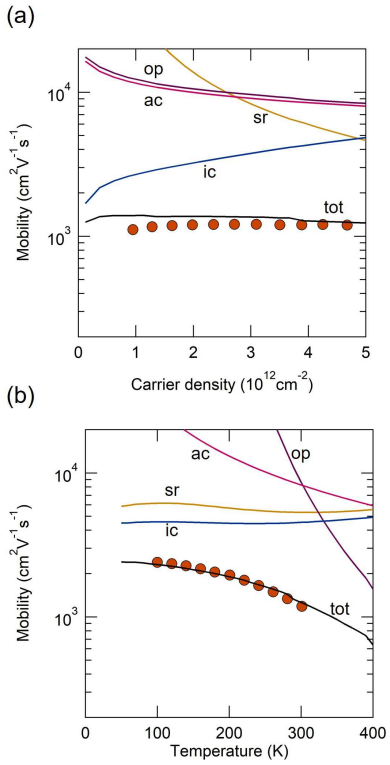

FIG. 4. Theoretical analysis of mobility. (a) Carrier density dependence and (b) temperature dependence of mobility. Red circles show experimental results for sample B1. The carrier density dependence was measured at 300 K. The temperature dependence was measured with an applied gate voltage of −6 V. Solid lines show the results of the theoretical calculation of mobility. The labels "ic," "sr," "ac," and "op" indicate the calculated mobilities limited by interface charges, surface roughness, acoustic phonon, and optical phonon, respectively. The mobility limited by background impurity scattering has values much higher than the plot range. The label "tot" indicates the calculated mobility considering all the above scattering.